

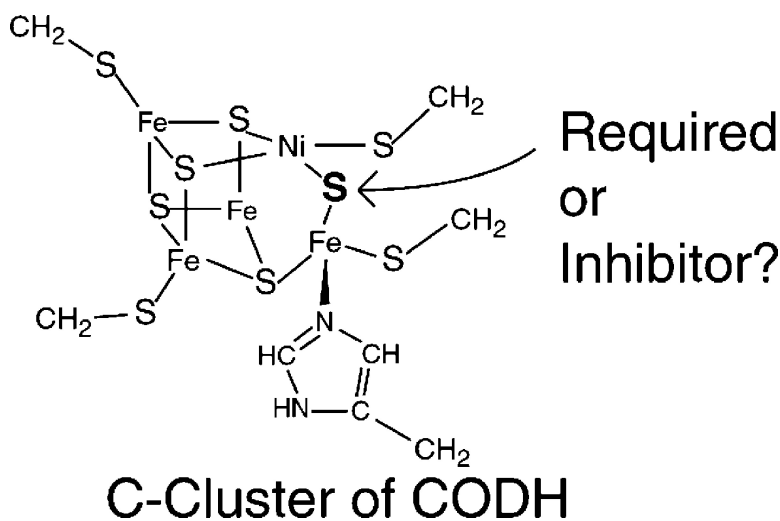
Article

**Effect of Sodium Sulfide on Ni-Containing Carbon Monoxide Dehydrogenases**

Jian Feng, and Paul A. Lindahl

*J. Am. Chem. Soc.*, **2004**, 126 (29), 9094-9100 • DOI: 10.1021/ja048811g • Publication Date (Web): 23 June 2004

Downloaded from <http://pubs.acs.org> on March 31, 2009



**More About This Article**

Additional resources and features associated with this article are available within the HTML version:

- Supporting Information
- Links to the 1 articles that cite this article, as of the time of this article download
- Access to high resolution figures
- Links to articles and content related to this article
- Copyright permission to reproduce figures and/or text from this article

[View the Full Text HTML](#)



**ACS Publications**  
 High quality. High impact.

## Effect of Sodium Sulfide on Ni-Containing Carbon Monoxide Dehydrogenases

Jian Feng<sup>†</sup> and Paul A. Lindahl<sup>\*,†,‡</sup>

Departments of Chemistry and of Biochemistry and Biophysics, Texas A&M University,  
College Station, Texas 77843-3255

Received March 2, 2004; E-mail: Lindahl@mail.chem.tamu.edu

**Abstract:** The structure of the active-site C-cluster in CO dehydrogenase from *Carboxydotherrmus hydrogenoformans* includes a  $\mu^2$ -sulfide ion bridged to the Ni and unique Fe, whereas the same cluster in enzymes from *Rhodospirillum rubrum* (CODH<sub>Rr</sub>) and *Moorella thermoacetica* (CODH<sub>Mt</sub>) lack this ion. This difference was investigated by exploring the effects of sodium sulfide on activity and spectral properties. Sulfide partially inhibited the CO oxidation activity of CODH<sub>Rr</sub> and generated a lag prior to steady-state. CODH<sub>Mt</sub> was inhibited similarly but without a lag. Adding sulfide to CODH<sub>Mt</sub> in the C<sub>red1</sub> state caused the  $g_{av} = 1.82$  EPR signal to decline and new features to appear, including one with  $g = 1.95, 1.85$  and  $(1.70$  or  $1.62)$ . Removing sulfide caused the  $g_{av} = 1.82$  signal to reappear and activity to recover. Sulfide did not affect the  $g_{av} = 1.86$  signal from the C<sub>red2</sub> state. A model was developed in which sulfide binds reversibly to C<sub>red1</sub>, inhibiting catalysis. Reducing this adduct causes sulfide to dissociate, C<sub>red2</sub> to develop, and activity to recover. Using this model, apparent  $K_i$  values are  $40 \pm 10$  nM for CODH<sub>Rr</sub> and  $60 \pm 30$   $\mu$ M for CODH<sub>Mt</sub>. Effects of sulfide are analogous to those of other anions, including the substrate hydroxyl group, suggesting that these ions also bridge the Ni and unique Fe. This proposed arrangement raises the possibility that CO binding labilizes the bridging hydroxyl and increases its nucleophilic tendency toward attacking Ni-bound carbonyl.

Ni-containing carbon monoxide dehydrogenases are found in anaerobic bacteria and archaea that grow autotrophically on CO or CO<sub>2</sub> and reducing equivalents.<sup>1</sup> They contain a novel Ni–Fe–S cluster called the *C-cluster* that serves as the active site for the reversible oxidation of CO to CO<sub>2</sub> (reaction 1, where MV refers to the commonly used in vitro electron acceptor/donor methyl viologen).



X-ray crystal structures of enzymes from 3 organisms, including *Carboxydotherrmus hydrogenoformans* (CODH<sub>Ch</sub>), *Rhodospirillum rubrum* (CODH<sub>Rr</sub>), and *Moorella thermoacetica* (CODH<sub>Mt</sub>) have been published, including two independent structures for CODH<sub>Mt</sub>.<sup>2–5</sup> CODH<sub>Ch</sub> and CODH<sub>Rr</sub> are  $\beta_2$  homodimers with molecular masses of 120–140 kDa, whereas CODH<sub>Mt</sub> is a 310 kDa  $\alpha_2\beta_2$  tetramer. The  $\alpha$  subunits of CODH<sub>Mt</sub> catalyze another reaction not catalyzed by the other two enzymes, namely the synthesis of acetyl-CoA. The four  $\beta_2$  structures are essentially equivalent, in that each  $\beta$  subunit contains 1 C-cluster and 1

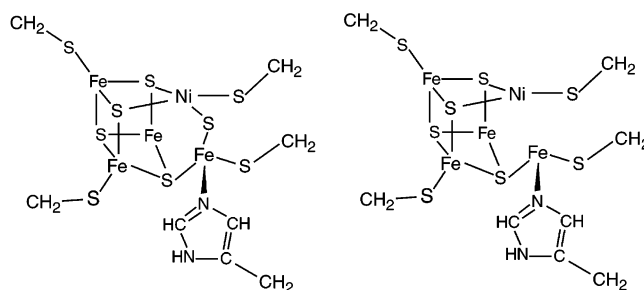


**Figure 1.** C-cluster structures. The structure on the left was reported for CODH<sub>Ch</sub>,<sup>2</sup> whereas that on the right represents those structure reported for CODH<sub>Mt</sub> and CODH<sub>Rr</sub>.<sup>3–5</sup> Other differences between the four structures are not highlighted.

[Fe<sub>4</sub>S<sub>4</sub>]<sup>2+/1+</sup> *B-cluster*. Another Fe<sub>4</sub>S<sub>4</sub> cubane called the *D-cluster* bridges the two  $\beta$  subunits. B- and D-clusters transfer electrons between the C-cluster and external redox agents.

Reported structures of the C-cluster are similar but not identical. The C-cluster in CODH<sub>Ch</sub> consists of 1 Ni, 4 Fe, and 5 sulfide ions (Figure 1, left). Three irons and 4 sulfide ions are organized as an [Fe<sub>3</sub>S<sub>4</sub>] subsite, while the Ni and remaining Fe can be viewed as a [Ni Fe] subsite bridged by a  $\mu^2$ -bridging sulfide ion. Structures of the other three C-clusters lack this sulfide ion, as shown in Figure 1, right. There are other potentially important differences between these structures but these will not be discussed here.

The C-cluster can be stabilized in four redox states, called C<sub>ox</sub>, C<sub>red1</sub>, C<sub>int</sub>, and C<sub>red2</sub>.<sup>6–9</sup> The fully oxidized C<sub>ox</sub> state is S = 0 and appears not to be involved in CO/CO<sub>2</sub> redox catalysis. Reduction by 1 electron to the S = 1/2 C<sub>red1</sub> state activates the

<sup>†</sup> Department of Chemistry.

<sup>‡</sup> Department of Biochemistry and Biophysics.

- (1) Lindahl, P. A. *Biochemistry* **2000**, *41*, 2097–2105.
- (2) Dobbek H.; Svetlitchnyi, V.; Gremer, L.; Huber, R.; Meyer, O. *Science* **2001**, *293*, 1281–1285.
- (3) Drennan, C. L.; Heo, J.; Sintchak, M. D.; Schreiter, E.; Ludden, P. W. *Proc. Natl. Acad. Sci. U.S.A.* **2001**, *98*, 11 973–11 978.
- (4) Doukov, T. L.; Iverson, T. M.; Saravalli, J.; Ragsdale, S. W.; Drennan, C. L. *Science* **2002**, *298*, 567–572.
- (5) Darnault, C.; Volbeda, A.; Kim, E. J.; Legrand, P.; Vernede, X.; Lindahl P. A.; Fontecilla-Camps, J. C. *Nature Structural Biology* **2003**, *10*, 271–279.

enzyme.<sup>10</sup> During catalysis, CO probably coordinates to the Ni of the C-cluster in this state, followed by the attack of the carbonyl by a hydroxide ion, forming a Ni-bound carboxylate. The  $S = 1/2$   $C_{red2}$  state then forms as  $CO_2$  dissociates. The C-cluster in the  $C_{red2}$  state transfers 2 electrons, in 1-electron steps, to the B- and D-clusters. In doing so, it passes through an EPR-silent  $C_{int}$  state,<sup>9</sup> and ultimately returns to the  $C_{red1}$  state.<sup>7</sup>

We were intrigued by the  $\mu^2$ -sulfide ion uniquely found in the  $CODH_{Ch}$  C-cluster, and endeavored to understand the circumstances for its presence. One possibility was that this sulfide ion is required for catalysis and that the 3 structures lacking it might reflect enzyme crystallized in an inactive form. Alternatively, the sulfide ion might inhibit catalysis and  $CODH_{Ch}$  might have been crystallized in an inactive form. Other possibilities are that the C-cluster in  $CODH_{Ch}$  might differ intrinsically from those in the other enzymes, or that the sulfide ion might only bind to a particular C-cluster redox state. In this study, we address these issues by examining the effect of sulfide ion on the activity and spectral properties of  $CODH_{Mt}$  and  $CODH_{Rr}$ . Our results indicate that added sulfide ion *inhibits* catalysis and binds to the  $C_{red1}$  state but not to the  $C_{red2}$  state of the C-cluster. Implications for the structure of the C-cluster and mechanism of catalysis are discussed.

## Experimental Procedures

**General Procedures** *R. rubrum* and *M. thermoacetica* cells were grown as described.<sup>10,11</sup>  $CODH_{Rr}$  and  $CODH_{Mt}$  were purified anaerobically as described.<sup>10–12</sup> Protein concentrations, CO oxidation activities, electrochemical potential measurements, and stopped-flow experiments were performed as described.<sup>10</sup> Unless mentioned otherwise, experiments involving protein manipulations were performed in an Ar-atmosphere glovebox (Vacuum/Atmospheres, Inc.) containing less than 1 ppm  $O_2$  as monitored continuously by an analyzer (Teledyne Analytical Instruments, model 310). EPR experiments were performed using a Bruker EMX spectrometer using ER4116DM (dual mode) and ER4102ST (standard mode) cavities and an Oxford Instruments ESR900 continuous flow cryostat. CO oxidation activities are reported as  $v_0/[E]_{tot}$  where  $v_0$  refers to initial steady-state rates ( $\mu M$  CO oxidized per min) in rate-vs-time plots that lacked lag periods, or to steady-state rates immediately after lag periods, in plots that contained lags.  $[E]_{tot}$  in  $\mu M$  were converted from mg/mL values by assuming molecular masses of 62 000 da for each  $\beta$  subunit of  $CODH_{Rr}$ <sup>12</sup> and 155,000 da for each  $\alpha\beta$  dimer of  $CODH_{Mt}$ .<sup>13</sup>

**Experiment of Figure 2: Effect of Sulfide with  $CODH_{Rr}$  on CO Oxidation Activity.** A 5.0 mM solution of sodium sulfide (Sigma) was prepared in 0.1 N NaOH. A portion of this stock was added to 1.0 mL of  $CODH_{Rr}$  ( $0.38 \mu M \beta$ , final concentration in buffer A, defined as 100 mM MOPS, pH 7.5) such that the final concentration of sulfide was  $200 \mu M$ . Another

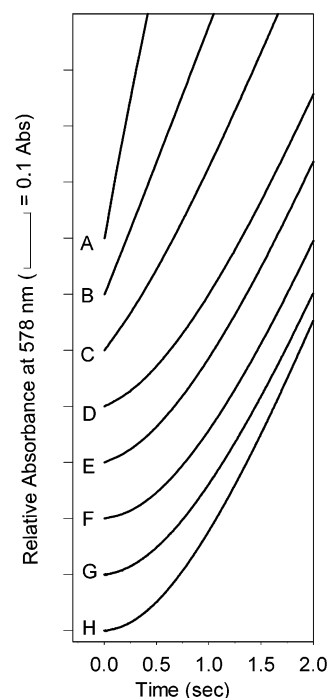


**Figure 2.** CO oxidation activity of  $CODH_{Rr}$  in the presence of sodium sulfide. Assays were performed as described in Experimental Procedures. Final concentrations of sulfide ion (in  $\mu M$ ) were as follows: A, 0; B, 0.25; C, 0.5; D, 1.25; E, 2.5; F, 5; G, 10; H, 100. Displayed traces are the average of three experimental traces. Each trace began at ca. 0.02 AU. Traces B–H are offset by 0.1 AU increments in the figure.

portion of the stock solution was diluted 10:1 with buffer A and aliquots were added to  $CODH_{Rr}$  as above, resulting in solutions with 5.0, 10, and  $20 \mu M$  sulfide. A final portion of the stock solution was diluted 100:1 with buffer A, and aliquots were added to  $CODH_{Rr}$  as above, resulting in solutions with 0, 0.5, 1.0 and  $2.5 \mu M$  of sulfide. These 8 solutions of  $CODH_{Rr}$ /sulfide were incubated 30 min, and then each was loaded into a stopped-flow syringe as described.<sup>10</sup> The other syringe contained CO oxidation assay buffer (20 mM methyl viologen (MV) in buffer A equilibrated with 1 atm CO). Each solution was assayed for CO oxidation activity one-by-one such that the last of the 8 solutions was assayed ca. 40 min after the first was assayed. Reactions were at  $30^\circ C$  and monitored in PM mode with 0.15 cm path length at 578 nm ( $\epsilon = 9.8 \text{ mM}^{-1}\text{cm}^{-1}$ ). As a result of stopped-flow mixing, final concentrations of sulfide,  $CODH_{Rr}$  and MV are half of those in premixed solutions.

**Experiments of Figures 3 and 4: EPR Studies.**  $CODH_{Mt}$  was freed of dithionite by passage through a column of  $1.6 \times 30$  cm Sephadex G-25 equilibrated in buffer B (50 mM Tris-HCl buffer pH 8), then concentrated with a centricon (YM50, Millipore) and transferred to a quartz UV-vis cuvette. While monitoring at 600 nm, sufficient 1.0 mM thionin in Buffer B was added to cause the absorbance to increase (due to unreacted oxidized thionin). The protein was removed from the cuvette, concentrated using a centricon and separated into 10  $130 \mu L$  aliquots of  $CODH_{Mt}$ . One aliquot was mixed with  $120 \mu L$  of buffer B and transferred to an EPR tube, affording sample a (final volume,  $250 \mu L$ ). A 100 mM stock solution of sodium sulfide in 0.1 N NaOH was prepared. Two other  $CODH_{Mt}$  aliquots were mixed with 12.5 and  $25 \mu L$  of the stock sulfide solution and with 107.5 and  $95 \mu L$  of buffer B, respectively,

- (6) Lindahl, P. A.; Münck, E.; Ragsdale, S. W. *J. Biol. Chem.* **1990**, *265*, 3873–3879.  
 (7) Anderson, M. E.; Lindahl, P. A. *Biochemistry* **1996**, *35*, 8371–8380.  
 (8) Hu, Z.; Spangler, N. J.; Anderson, M. E.; Xia, J. Q.; Ludden, P. W.; Lindahl, P. A.; Münck, E. *J. Am. Chem. Soc.* **1996**, *118*, 830–845.  
 (9) Fraser, D. M.; Lindahl, P. A. *Biochemistry* **1999**, *38*, 15706–15711.  
 (10) Feng, J.; Lindahl, P. A. *Biochemistry* **2004**, *43*, 1552–1559.  
 (11) Shin, W.; Stafford, P. R.; Lindahl, P. A. *Biochemistry* **1992**, *31*, 6003–6011.  
 (12) Bonam, D.; Ludden, P. W. *J. Biol. Chem.* **1987**, *262*, 2980–2987.  
 (13) Morton, T. A.; Runquist, J. A.; Ragsdale, S. W.; Shanmugasundaram, T.; Wood, H. G.; Ljungdahl, L. G. *J. Biol. Chem.* **1991**, *266*, 23824–23828.

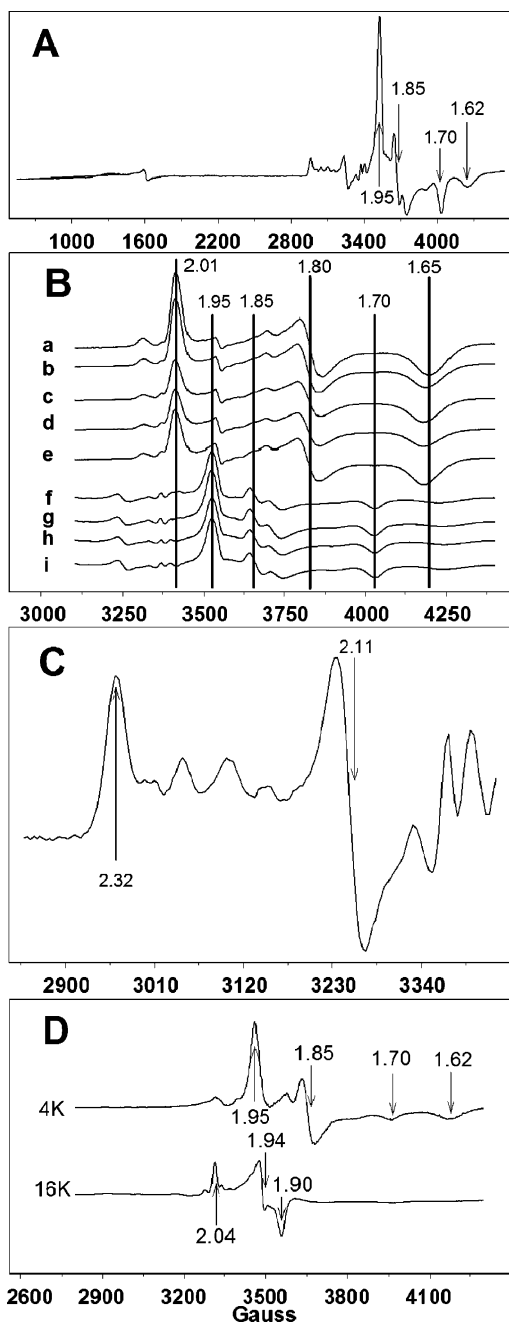


**Figure 3.** Effect of sodium sulfide on  $C_{red1}$  EPR spectra from  $CODH_{Mt}$ .  $CODH_{Mt}$  ( $130 \mu M \alpha\beta$  poised with the C-cluster in the  $C_{red1}$  state as described in Experimental Procedures) was treated with sodium sulfide at the following concentrations (in  $\mu M$ ). Panel A, 10 000; Panel B, (a) 0; (b) 1; (c) 10; (d) 50; (e) 100; (f) 500; (g) 1000; (h) 5000; (i) 10 000 (same sample as for Panel A). EPR conditions: Modulation amplitude, 10 G; microwave frequency, 9.600 GHz; microwave power, 20 mW; dual-mode cavity; temperature, 10 K. Panel C, same as trace g Panel B, showing close up of minority features. Panel D, same as in Panel C, but obtained at 4 and 16 K. EPR conditions as above except that the microwave frequency was 9.450 GHz and the standard cavity was used.

and then transferred to EPR tubes to afford samples h and i, respectively. A portion of the stock solution was diluted 10:1 with buffer B, and 12.5 and 25  $\mu L$  were used in preparing samples f and g. Another portion of stock solution was diluted 100:1, and 0.25, 2.5, 12.5, and 25  $\mu L$  were used to prepare samples b, c, d, and e. A 50 mM solution of dithionite in 0.1 N NaOH was freshly prepared, and 10  $\mu L$  were mixed with the last  $CODH_{Mt}$  aliquot and 85  $\mu L$  Buffer B. After 20 min

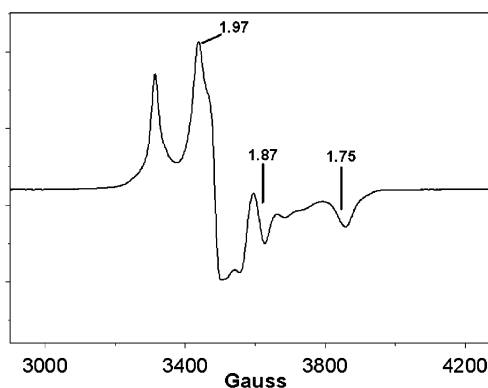


**Figure 4.** EPR spectrum of  $CODH_{Mt}$  poised in the  $C_{red2}$  state. Sodium sulfide was 1 mM. Refer to Figure 7B of ref 7 for a control  $C_{red2}$  spectrum. EPR conditions were as in Figure 3, Panel B.

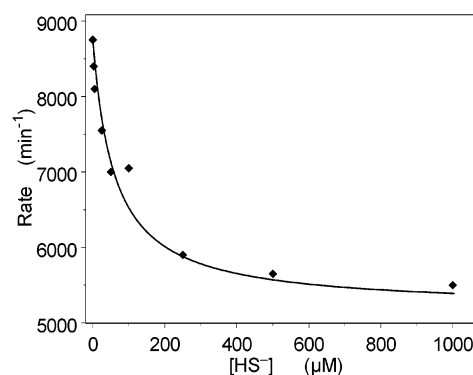


**Figure 5.** CO oxidation activity of  $CODH_{Mt}$  preincubated in sodium sulfide. Assays were performed as described in Experimental Procedures. Final concentrations of sulfide ion (in  $\mu M$ ) were 0, 2.5, 5, 25, 50, 100, 250, 500, 1000. Activities are given in Table 1 and the solid line is a simulation using eq 14 with  $K_I = 60 \mu M$ . Reaction rates were determined from the linear regions of absorbance traces, including 4–4.5 s for 0, 2.5, 5, 25, 50, 100  $\mu M$  samples, and 19–20 s for 250, 500, 1000  $\mu M$  samples.

incubation, 25  $\mu L$  of the 10:1 diluted sulfide solution was added, affording the 250  $\mu L$  EPR sample of Figure 4. All samples were incubated for ca. 30 min after sulfide was added, sealed with rubber septa, removed from the box and frozen immediately in  $LN_2$ .

**Experiment of Figure 5: Effect of Sulfide with  $CODH_{Mt}$  on CO Oxidation Activity.** A 100 mM stock solution of sodium sulfide was prepared in 0.1 N NaOH. A portion of this stock was diluted 10:1 with buffer B and 6–240  $\mu L$  aliquots were mixed with 1074–840  $\mu L$  of buffer B and 120  $\mu L$  of  $CODH_{Mt}$  (35 nM  $\alpha\beta$  after mixing), resulting in 1.2 mL solutions with 50, 100, 200, 500, 1000, and 2000  $\mu M$  sulfide. Another portion of the stock was diluted 100:1 with buffer B and 0–12  $\mu L$  aliquots were added to 1068–1080  $\mu L$  of buffer B and 120  $\mu L$  of  $CODH_{Mt}$ , resulting in solutions with 0, 5.0 and 10  $\mu M$  sulfide. After ca. 30 min incubation, the resulting 9 solutions were assayed for CO oxidation activity as in the Figure 2 experiment except that the CO oxidation assay solution contained buffer B rather than buffer A, and reactions were monitored at 604 nm ( $\epsilon = 13.9 \text{ mM}^{-1} \text{ cm}^{-1}$ ) with a 1 cm path length.

**Experiment of Figure 6: Irrelevance of Preincubation on Sulfide Inhibition.** A 60 mL Wheaton vial was sealed with a rubber septum in the glovebox and its Ar atmosphere was replaced with 1 atm CO using a Schlenk line. After returning the vial into the glovebox, 4.0 mL of buffer A containing 35 nM  $\alpha\beta$   $CODH_{Mt}$  and 10  $\mu M$  MV were injected into the vial.

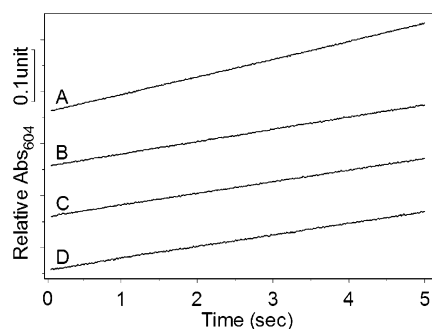


**Figure 6.** Stopped-flow traces showing the irrelevance of preincubation on sulfide inhibition. See Experimental Procedures for details. Incubation times: A, no sulfide present; B, 0.015 s; C, 60 s; D, 500 s. Traces have been shifted from each other by 0.1 absorbance units for clarity.

The contents were incubated for 5 min, and then 0.8 mL of the resulting CO-saturated solution was loaded into the stopped-flow drive syringe A as described.<sup>10</sup> Syringe B was loaded with a freshly prepared solution of 2 mM sodium sulfide in buffer A. This solution had been prepared by mixing 40  $\mu\text{L}$  of a 100 mM sodium sulfide plus 100 mM NaOH solution into 1960  $\mu\text{L}$  of buffer A. In the control experiment, syringe B was filled with buffer A alone. Syringe C was loaded with 20 mM MV in buffer A. In the control experiment, syringes A and B were mixed for 0.015 s and then reacted with syringe C. In the other experiments, syringes A and (sulfide-containing) syringe B were mixed for 0.015, 60 and 500 s before reacting with syringe C. After all mixings,  $[\text{CODH}_{\text{Mt}}] = 8.7 \text{ nM}$ ,  $[\text{CO}] = 220 \mu\text{M}$ ,  $[\text{MV}] = 10 \text{ mM}$ , and  $[\text{HS}^-] = 500 \mu\text{M}$ . CO oxidation activity assays were performed at 30° C and monitored at 604 nm.

**Reversibility of Sulfide Inhibition.** An aliquot of  $\text{CODH}_{\text{Mt}}$  (10  $\mu\text{L}$  of 84  $\mu\text{M}$   $\alpha\beta$ ) was assayed as in the Figure 5 experiment, while the remainder (1.0 mL) was mixed with 10  $\mu\text{L}$  of a freshly prepared 600 mM stock solution of sodium sulfide in 0.1 N NaOH. After incubating for 40 min, a 10  $\mu\text{L}$  aliquot of the resulting  $\text{CODH}_{\text{Mt}}$  solution with 6.0 mM sulfide was assayed for activity. The remaining solution was divided into two 0.5 mL portions, one of which was reacted with 2  $\mu\text{L}$  of 40 mM freshly made dithionite, the other of which was exposed to 1 atm CO. After incubating both for 1 h, solutions were passed individually through columns of Sephadex G25 (1  $\times$  15 cm for the CO-containing sample and 1  $\times$  30 cm for the dithionite-containing sample) that were equilibrated in buffer B. Eluted protein solutions were assayed as in the Figure 5 experiment.

Sample g from the EPR experiment of Figure 3 was thawed in the glovebox and mixed with 10  $\mu\text{L}$  of 50 mM freshly prepared dithionite. After incubating 30 min, the result solution was passed through a 1  $\times$  15 cm Sephadex G-25 column equilibrated in buffer B. The eluted solution was transferred into a quartz cuvette and titrated with 1 mM thionin as described for the experiment of Figure 3. The thionin-oxidized sample was concentrated to 250  $\mu\text{L}$  with a centricon unit, transferred to a clean EPR tube, sealed with a rubber septum, removed from the box and frozen immediately with  $\text{LN}_2$ .

**Experiment of Figure 7: Effect of CO on Enzyme Stability.** A 350  $\mu\text{L}$  stock solution of 16.3 mg/mL  $\text{CODH}_{\text{Mt}}$  was separated into 7  $\times$  50  $\mu\text{L}$  aliquots and transferred into glass tubes (5  $\times$  45 mm, Fisher). Tubes were sealed with rubber septa (which had been stored in the box for > 1 month), then removed from the box. On a Schlenk line with needle outputs, tube

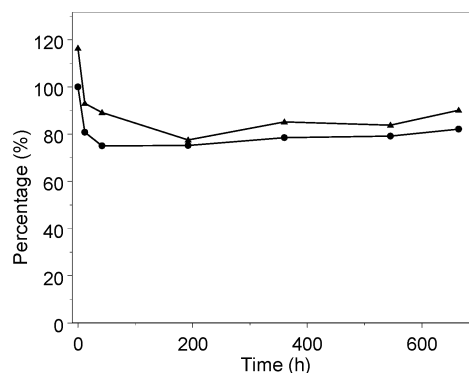


**Figure 7.** Effect of incubating CO with  $\text{CODH}_{\text{Mt}}$  on CO oxidation activities. Triangles,  $\text{CODH}_{\text{Mt}}$  in 1 atm CO (initial activity = 16 500  $\text{min}^{-1}$ ). Circles,  $\text{CODH}_{\text{Mt}}$  in 1 atm Ar (initial activity = 14,400  $\text{min}^{-1}$ ). See Experimental Procedures for details. Percentage of activity plotted is relative to control activity at  $t = 0$ .

headspaces were replaced with 1 atm of prepurified-grade CO which had been scrubbed for  $\text{O}_2$  using an Oxisorb (Messer) cartridge. Septa were wrapped tightly with electronic tape; then tubes were transferred to an Ar-atmosphere glovebox (MBraun, Inc.) maintained at 4 °C and at <1 ppm  $\text{O}_2$ . As a control, 200  $\mu\text{L}$  of the stock solution was transferred into a similar tube and sealed with a septum (i.e. with an Ar headspace). At time  $t = 0$ , aliquots of the control and 1 CO-treated sample were removed from the box and assayed for CO oxidation activity as described.<sup>11</sup> Similar assays were performed at various times, using a different CO-treated aliquot at each time (minimizing CO leakage caused by punctured septa). After  $t = 664 \text{ h}$ , 20  $\mu\text{L}$  of assay buffer without CO (50 mM Tris plus 20 mM  $\text{MV}^{2+}$ ) was injected into the CO-treated sample which had been assayed at  $t = 0$ . The solution immediately turned dark blue, indicating the presence of CO in that sample 664 h after it was prepared. In contrast, the Ar-treated control showed no evidence of turning blue indicating the absence of CO in the control sample 664 h after it was prepared.

## Results

Adding sodium sulfide to  $\text{CODH}_{\text{R}}$  attenuated steady-state CO oxidation activity (Figure 2). Although there are multiple equilibria involving sulfide ions in aqueous solution at neutral pH, with  $\text{HS}^-$  the predominant species,<sup>14</sup> we will refer to all species collectively as *sulfide* ions. Activities declined with increasing amounts of added sulfide ion, but not to zero activity even at the highest concentrations used. In the absence of sulfide, no lag phase was evident. Electrochemical potentials of the  $\text{CODH}_{\text{R}}$  solutions used in these experiments ranged from  $-210 \text{ mV}$  to  $-310 \text{ mV}$  vs NHE. These potentials and the absence of a lag phase are consistent with the C-clusters in these  $\text{CODH}_{\text{R}}$  samples being in the  $\text{C}_{\text{red1}}$  state at the time of injection.<sup>10</sup> Equivalent samples to which sodium sulfide was added exhibited a lag phase. The length of this lag increased with increasing sulfide ion concentration, reaching a maximum of  $\sim 1/2 \text{ sec}$ .

Samples of  $\text{CODH}_{\text{Mt}}$  were freed from dithionite and oxidized with a slight excess of thionin. In this state only the  $g_{\text{av}} = 1.82$

(14) Weast, R. C., ed. (1986) Handbook of Chemistry and Physics, 66<sup>th</sup> edition, CRC Press, Boca Raton, FL. The predominance of  $\text{HS}^-$  is evident by applying the  $\text{pK}'\text{s}$  of  $\text{H}_2\text{S}$  given in this reference (7.04 and 11.96) to the Henderson–Hasselbalch equation.



does not bind to the  $C_{red2}$  state. The sulfide-bound  $[Ni^{2+}-HS^- - Fe^{2+}]$  state ( $C_{red1}:S$ ) can be reduced to yield  $C_{red2}$  and free sulfide ion. Without this last assumption, the observed residual activity in the presence of excess sulfide ion could not be explained simply.

The model can be simplified further and used to analyze our data by assuming that  $[CO]$ ,  $[OH^-]$ ,  $[H^+]$  and  $[MV^{2+}]$  are invariant during the reaction. If the measured product of catalysis is called "P" rather than  $2MV^{1+}$ , the model becomes reactions 2–6.



The differential equations for  $d[C_{red1}]/dt$ ,  $d[C_{red2}]/dt$ , and  $d[C_{red1}:S]/dt$  as generated from these reactions were equated to zero according to the steady-state assumption and solved for  $C_{red2}$  using relationship  $[C_{red1}:S] = [C_{tot}] - [C_{red1}] - [C_{red2}]$ . The reaction velocity at steady state is

$$v = \frac{d[P]}{dt} = k_2[C_{red2}] = \frac{k_2(k_1k_4 + k_3k_5[HS^-] + k_1k_5)[C_{tot}]}{k_1k_4 + k_1k_5 + k_2k_4 + k_3k_5[HS^-] + k_2k_3[HS^-] + k_2k_5} \quad (7)$$

In the absence of sulfide ion,  $[HS^-] = 0$  and eq 7 becomes

$$v_{max} = \frac{k_1k_2[C_{tot}]}{k_1 + k_2} \quad (8)$$

while in the limit as  $[HS^-]$  approaches infinity, eq 7 becomes

$$v_{min} = \frac{k_2k_5[C_{tot}]}{k_2 + k_5} \quad (9)$$

From the data of Table 1,  $v_{max} = 102\,900\text{ min}^{-1}$ ,  $v_{min} = 39\,900\text{ min}^{-1}$ , and  $[C_{tot}] = 0.19\text{ }\mu\text{M}$ . Substituting these values into [8] and [9], and solving for  $k_1$  and  $k_5$  yields

$$k_1 = \frac{10\,290\,000k_2}{19k_2 - 10\,290\,000} \text{ and } k_5 = \frac{210\,000k_2}{k_2 - 210\,000} \quad (10,11)$$

The sulfide concentration which yielded the reaction velocity midway between  $v_{max}$  and  $v_{min}$  was equated to the apparent dissociation constant  $K_1$  for sulfide binding, yielding

$$K_1 = [HS^-]_{(ave = (v_{max} + v_{min})/2)} = \frac{k_1k_4 + k_1k_5 + k_2k_4 + k_2k_5}{k_3(k_2 + k_5)} \quad (12)$$

Substituting this relationship, as well as those for  $k_1$  and  $k_5$  into eq 7 yields

$$v = \frac{102\,900K_1 + 39\,900[HS^-]}{K_1 + [HS^-]} \quad (13)$$

Pairs of values  $\{v, [HS^-]\}$  given in Table 1 were substituted into eq 13 and the resulting relationships were solved for  $K_1$ , yielding the average value  $40 \pm 10\text{ nM}$ .

Applying the same model to  $CODH_{Mt}$  and analysis as was used for  $CODH_{Rr}$  afforded the rate equation

$$v = \frac{8750K_1 + 5190[HS^-]}{K_1 + [HS^-]} \quad (14)$$

The value of  $K_1$  was again adjusted to fit the data of Table 1, yielding  $K_1 = 60 \pm 30\text{ }\mu\text{M}$ . Thus, sulfide ion binds more tightly to  $CODH_{Rr}$  than it does to  $CODH_{Mt}$ . This difference in binding strength may explain the absence of a lag phase in the  $CODH_{Mt}$  experiment. It is also congruent with the somewhat higher concentrations of sulfide required for there to be noticeable effects in  $CODH_{Mt}$  EPR spectra than were required to observe effects in activity of  $CODH_{Rr}$ .

## Discussion

It is simplest to assume that sulfide ion inhibits CO oxidation catalysis by binding to the C-cluster in the manner evident in the structure of Dobbek et al.<sup>2</sup>—i.e., bridging the Ni and the unique Fe (Figure 1, left-hand side). The ability of sulfide to bind to the  $C_{red1}$  state but not to  $C_{red2}$  suggests that  $CODH_{Ch}$  may have been crystallized in the  $C_{red1}S$  state (or in the  $C_{ox}$  or  $C_{int}$  states, as we have no information as to whether sulfide binds these states of the C-cluster), and that the other structures may have been crystallized in more reduced states such as  $C_{red2}$ . Given our evidence that sulfide ion is a dissociable inhibitor, the intrinsic structure of the C-cluster would be that of Figure 1, right-hand side.

The effect of sulfide ion on CODH activity and spectral properties are qualitatively similar to those of other anions, including cyanide, cyanate, thiocyanate, and azide ions.<sup>15–17</sup> Cyanide ion fully inhibits CODH's, apparently by binding to the  $C_{red1}$  state as evidenced by a shift in the  $C_{red1}$  EPR signal when  $CN^-$  is added.<sup>15</sup> This effect can be reversed (i.e., activity recovers fully and the EPR signal converts to that from  $C_{red2}$ ) when  $CN^-$ -treated enzyme is incubated in CO for ca. 1 h. Also, pretreatment with CO protects the enzyme from the effects of  $CN^-$ , apparently by maintaining it in the  $C_{red2}$  state. Thus, it appears that this anion does not bind to the  $C_{red2}$  state. Thiocyanate, cyanate and azide also appear to bind  $C_{red1}$  but not  $C_{red2}$ .<sup>16,17</sup> Similar to sulfide, inhibition by thiocyanate is partial.<sup>16</sup> This reactivity pattern common to sulfide and other inhibitory anions suggests that these other anions might also bind to the enzyme in the same manner as sulfide—i.e., bridging the Ni and unique Fe of the C-cluster.

Binding of  $CN^-$  shifts the position of Ferrous Component II in Mössbauer spectra<sup>8</sup> which corresponds to the unique Fe of

(15) Anderson, M. E.; Lindahl, P. A. *Biochemistry* **1994**, *33*, 8702–8711.

(16) Seravalli, J.; Kumar, M.; Lu, W. P.; Ragsdale, S. W. *Biochemistry* **1995**, *34*, 7879–7888.

(17) Seravalli, J.; Kumar, M.; Lu, W.-P.; Ragsdale, S. W. *Biochemistry* **1997**, *36*, 11 241–11 251.

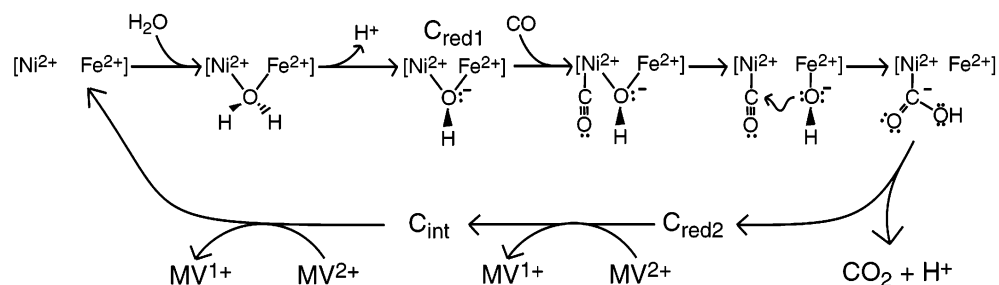


**Figure 9.** Mechanism of catalysis, emphasizing a proposed  $\mu^2$ -bridging hydroxyl group and CO-induced labilization. See text for details.

the C-cluster. This suggests that  $\text{CN}^-$  binds to the unique Fe; whether it also binds, in bridging fashion, to the Ni would not have been evident from the Mössbauer experiments. With  $\text{CN}^-$  bound, added CO cannot reduce the enzyme's Fe-S clusters, suggesting that CO does not oxidize to  $\text{CO}_2$  when  $\text{CN}^-$  is bound. Nevertheless, CO incubation can (somehow) accelerate the dissociation of  $\text{CN}^-$ .<sup>15</sup> One possibility is that CO binds to the C-cluster in the  $\text{C}_{\text{red1}}$  state with  $\text{CN}^-$  bound simultaneously, and that this binding encourages  $\text{CN}^-$  dissociation.<sup>15,18</sup> Initially, CO was thought to reactivate  $\text{CN}^-$ -inhibited CODHs noncompetitively by binding to a "modulator" site that was distinct from the C-cluster.<sup>15</sup> However, once it was understood that the C-cluster's spin density resided predominately on the Fe-S portion of the C-cluster rather than on the Ni, the modulator was proposed to be the Ni itself.<sup>7</sup> The presumed bridging mode for  $\text{CN}^-$  binding helps explain how CO binding to Ni might accelerate  $\text{CN}^-$  dissociation, in that CO binding might weaken Ni coordination to  $\text{CN}^-$  such that  $\text{CN}^-$  would become bound only to the unique Fe.

Using ENDOR spectroscopy, DeRose et al.<sup>19</sup> identified a strongly coupled proton associated with the  $\text{C}_{\text{red1}}$  state (but not with  $\text{C}_{\text{red2}}$ ) that was displaced by  $\text{CN}^-$ . Interpreting the proton as arising from the substrate hydroxide, this suggests that  $\text{CN}^-$  and  $\text{OH}^-$  bind at the same site. We were initially opposed to the idea that hydroxide bridges the Ni and unique Fe, because such binding would *deactivate* it in terms of nucleophilicity. However, such a bridging arrangement might also be required to deprotonate water at the appropriate  $\text{pK}_a$  for this reaction (i.e., coordination to Fe alone might not lower the  $\text{pK}_a$  sufficiently) or it might facilitate  $\text{OH}^-$  dissociation. A similar situation (water bridging two metal centers followed by deprotonation and nucleophilic attack) is evident in the enzyme arginase.<sup>20</sup> In this case, the hydroxide ion bridging two Mn(II) ions is an effective nucleophile for the hydrolysis reaction.

The connection between inhibitory anions and the substrate hydroxyl group suggests that they might bind similarly and share additional reactivity properties. First, hydroxide might also bind to  $\text{C}_{\text{red1}}$  (or more accurately, bind to an unnamed state of the C-cluster that becomes  $\text{C}_{\text{red1}}$  once the hydroxide is bound) but not to  $\text{C}_{\text{red2}}$ , as supported by the ENDOR study. Second, CO binding may promote the dissociation of bound  $\text{OH}^-$  similarly to the way it promotes the dissociation of bound  $\text{CN}^-$ . This situation is depicted in Figure 9. Here, water binds in bridging mode to the Ni and unique Fe of the  $\text{C}_{\text{red1}}$  state. This lowers the  $\text{pK}_a$  of the water to the value observed—namely 7.2<sup>16</sup> and

results in a bridging hydroxyl group. When CO binds to the Ni, the Ni-OH bond breaks and a terminally bound HO-Fe species is formed. This weakly bound terminal hydroxyl group then dissociates from the Fe and attacks the carbonyl of Ni-bound CO. Thus, *CO-induced labilization might serve to increase the nucleophilic propensity of the hydroxyl group*. We find this an intriguing possibility that deserves further evaluation.

Finally, while this paper was being reviewed, another study was published by Meyer and co-workers in which the sulfide ion bridging the Ni and unique Fe in the  $\text{CODH}_{\text{Ch}}$  C-cluster was concluded to be *required* for activity.<sup>21</sup> This conclusion was based on a correlation between the presence/absence of this sulfide in X-ray crystal structures and the activity/inactivity of other samples treated similarly. In the presence of CO, their sample lost  $\sim 100\%$  activity in  $\sim 100$  hrs whereas in the absence of CO (under an  $\text{N}_2$  atmosphere),  $\sim 60\%$  of initial activity remained after the 100 hr incubation. The analogous experiment performed using  $\text{CODH}_{\text{Mt}}$  in our lab afforded significantly different results (Figure 7) which do not support the conclusion that CODH's are inactivated upon treatment with CO. We suspect that the absence of the bridging sulfide in their CO-treated samples arose because the C-cluster was in the  $\text{C}_{\text{red2}}$  state and would not support sulfide binding. The presence of bridging sulfide in samples prepared in the *absence* of low-potential reductants may have arisen because the C-cluster was in the  $\text{C}_{\text{red1}}$  state, and sufficient sulfide was present to bind and form the  $\text{C}_{\text{red1}}:\text{S}$  state. The presence of bridging sulfide in the sample prepared in the *presence* of dithionite is more difficult to explain, in that the C-cluster should have been in the  $\text{C}_{\text{red2}}$  state and unable to bind sulfide. However,  $\text{CODH}_{\text{Mt}}$  consumes dithionite spontaneously<sup>11</sup> raising the possibility that the dithionite-reduced sample was more oxidized than expected by the time it was exposed to X-rays. Despite differences in interpreting the role of the bridging sulfide in CODH catalysis, the results of Dobbek et al.<sup>21</sup> support our assumption that the sulfide bridging the Ni and unique Fe of a given C-cluster is labile and can bind/dissociate under appropriate conditions.

**Acknowledgment.** This work was supported by the National Institutes of Health (GM46441) and the Department of Energy (DE-FG03-01ER15177). The National Science Foundation supported the purchase of the EPR spectrometer (CHE-0092010). We thank Juan C. Fontecilla-Camps for suggesting (despite our initial objections) that the hydroxide ion used in catalysis might bridge the Ni and unique Fe of the C-cluster.

(18) Anderson, M. E.; DeRose, V. J.; Hoffman, B. M.; Lindahl, P. A. *J. Am. Chem. Soc.* **1993**, *115*, 12 204–12 205.

(19) DeRose, V. J.; Anderson, M. E.; Lindahl, P. A.; Hoffman, B. M. *J. Am. Chem. Soc.* **1998**, *120*, 8767–8776.

(20) Dismukes, G. C. *Chem. Rev.* **1996**, *96*, 2909–2926.

JA048811G

(21) Dobbek, H.; Svetlitchnyi, V.; Liss, J.; Meyer, O. *J. Am. Chem. Soc.* **2004**, *126*, 5382–5387.